

1 **Detrital zircon SHRIMP U-Pb age study of the Cordillera Darwin**  
2 **Metamorphic Complex of Tierra del Fuego: sedimentary sources**  
3 **and implications for the evolution of the Pacific margin of**  
4 **Gondwana**

5  
6  
7 F. Hervé<sup>\*1</sup>, C. M. Fanning<sup>2</sup>, R. J. Pankhurst<sup>3</sup>, C. Mpodozis<sup>4</sup>, K. Klepeis<sup>5</sup>, M.  
8 Calderón<sup>1</sup> & S. N. Thomson<sup>6</sup>

9  
10 1. Departamento de Geología, Universidad de Chile, Casilla 13518, Correo 21,  
11 Santiago, Chile.

12 2. Research School of Earth Sciences, Australian National University, Canberra,  
13 Australia

14 3. British Geological Survey, Keyworth, Nottingham NG12 5GG, United Kingdom

15 4. Enap-Sipetrol, (now at Antofagasta Minerals, Apoquindo 4001, Piso 18,  
16 Santiago, Chile)

17 5. Department of Geology, University of Vermont, Burlington, VT, 05405-0122,  
18 USA

19 6. Department of Geosciences, University of Arizona, Tucson, AZ 85721-0077,  
20 USA.

21  
22 \* Corresponding author (e-mail: [fherve@cec.uchile.cl](mailto:fherve@cec.uchile.cl))

23  
24 **Words:** 6900

25 **Figures:** 8

26 **Tables:** 0

27  
28 Supplementary material: Geographical coordinates of analysed samples, SHRIMP  
29 U-Th-Pb analytical data and representative cathodoluminescence (CL) images of  
30 zircon grains analysed are available at <http://www.geolsoc.org.uk/SUP00000>.

31  
32 Abbreviated title: Cordillera Darwin Zircon Dating

33  
34 **Abstract**

35  
36 The Cordillera Darwin Metamorphic Complex in the southernmost Andes includes  
37 a basement of probable Palaeozoic age, a mid-Jurassic and younger volcano-  
38 sedimentary cover, and a suite of Jurassic granites, all of which were jointly  
39 metamorphosed during the Cretaceous. Detrital zircon ages presented here show  
40 that some of the amphibolite facies metamorphic rocks previously mapped as  
41 basement have a Jurassic protolith. Overall the detrital zircon age patterns for

42 samples of the Cordillera Darwin basement differ from those of the Madre de Dios  
43 Terrane of the western Patagonian Andes with which they had been correlated;  
44 instead they are more comparable to those from the Eastern Andes Metamorphic  
45 Complex, which apparently developed in a passive margin setting. The paucity of  
46 Cambrian detrital zircons indicates that the meta-igneous basement of the  
47 Magallanes foreland basin of central and northern Tierra del Fuego was not the  
48 main source of detritus for the protolith of the Cordillera Darwin Metamorphic  
49 Complex. The possibility is envisaged that the Magallanes Fagnano transform fault  
50 boundary between the Scotia and South America plates resulted from reactivation  
51 of an older, pre-Jurassic suture zone between the basement terranes of north-  
52 central Tierra del Fuego and Cordillera Darwin.

53  
54  
55  
56  
57 Cordillera Darwin (Fig. 1) is the topographic culmination of the Fuegian Andes. Its  
58 core is occupied by the Cordillera Darwin Metamorphic Complex (CDMC, Kohn *et al.*  
59 *1995*), which includes a “basement unit” formed by metapelitic and  
60 metapsammitic rocks together with previously undated meta-igneous rocks, a  
61 cover of mainly rhyolitic volcanic rocks of the Upper Jurassic Tobífera Formation,  
62 and intrusive plutonic bodies of different ages. The main structural, metamorphic,  
63 intrusive and uplift history of Cordillera Darwin was revealed in a programme of  
64 pioneering field-work based research (Dalziel & Cortés 1972; Nelson *et al.* 1980;  
65 Dalziel 1981, 1986; Nelson 1982, among others). It was shown that both  
66 basement and cover were involved in deformation and metamorphism that also  
67 affected Late Jurassic granitoids of the Cordillera Darwin suite (Hervé *et al.* 1981;  
68 Mukasa & Dalziel 1986).

69 The CDMC is unique among the metamorphic complexes of the southern  
70 Andes in having a high metamorphic grade, resulting in kyanite- and sillimanite-  
71 bearing amphibolite facies rocks, notwithstanding the occurrence of amphibolite-  
72 facies metamorphic rocks containing staurolite and sillimanite elsewhere in  
73 southern Patagonia, at Puerto Eden (Watters 1964; Calderón *et al.* 2007a). The  
74 CDMC basement rocks may contain relicts of a pre-Andean fabric (Dalziel and  
75 Cortes 1972; Nelson *et al.*, 1980; Dalziel & Brown 1989), but according to Kohn *et al.*  
76 *(1995)* metamorphic conditions “evidently did not exceed lower greenschist  
77 grade prior to the Cretaceous”; these authors also established that peak high-  
78 grade metamorphism in the CDMC occurred between 90 and 100–120 Ma, based  
79 on stratigraphical relationships, K–Ar and Ar–Ar metamorphic mineral ages, and  
80 the ages of cross-cutting plutons.

81 The main deformation and high-grade metamorphism of the CDMC has been  
82 associated with the closure of the Rocas Verdes Basin (RVB) (Dalziel *et al.* 1974;  
83 Calderón *et al.* 2007b). Development of this quasi-oceanic extensional basin was  
84 synchronous with the initial stages of Gondwana break-up (Dalziel & Cortes 1972).  
85 The RVB was the depositional locus for the thick succession of Lower Cretaceous  
86 volcanoclastic sedimentary rocks of the Yaghan Formation (Katz & Watters 1966).  
87 Studies carried in the Ultima Esperanza region indicate that final closure of the

88 northern RVB uplift, ophiolite obduction, and flexural loading of the South  
89 American margin occurred after the Cenomanian (93 Ma) as shown by the age of  
90 detrital zircons in the first turbidites infilling the subsequent Magallanes foreland  
91 basin (Fildani *et al.* 2003).

92  
93  
94

#### 95 **Previous constraints on the age of the CDMC protolith**

96

97 The age and nature of the protolith of the CDMC basement is largely unknown. A  
98 depositional age can be constrained by regional stratigraphical relations with  
99 Mesozoic cover rocks. At Peninsula Staines, 350 km to the northwest of Cordillera  
100 Darwin, metamorphic rocks are unconformably overlain by the Middle to Upper  
101 Jurassic siliceous volcanic strata of the Tobífera Formation (Allen *et al.* 1980). The  
102 same stratigraphical relationship is seen in the northern slope of the Cordillera  
103 Darwin at Seno Almirantazgo (Dalziel & Cortés 1972), where Johnson (1990)  
104 described a succession of conglomerate and sandstone up to 80 m thick (Basal  
105 Clastic Complex, BCC), which overlies the basement with an erosional  
106 unconformity, and concordantly underlies Tobífera Formation volcanic rocks. A  
107 Rb–Sr whole rock errorchron of  $240 \pm 40$  ( $2\sigma$ ) Ma was obtained for metamorphic  
108 rocks from Bahía Pluschow belonging to the basement unit by Hervé *et al.* (1981).  
109 Kohn *et al.* (1995) suggested that the CDMC basement corresponds to a  
110 Palaeozoic to lower Mesozoic (?) metasedimentary and metavolcanic unit,  
111 believed to have been originally deposited as an accretionary wedge on the pre-  
112 Mid Jurassic Pacific margin of South America (Dalziel & Cortés 1972; Nelson *et al.*  
113 1980; Dalziel 1981, 1986). An alternative possibility has been suggested recently  
114 (Hervé *et al.* 2008), that it might be correlative with the Eastern Andes  
115 Metamorphic Complex, deposited in a passive margin environment and cropping  
116 out in the Patagonian Andes inboard of the Patagonian Batholith.

117 Barbeau *et al.* (2009) analysed detrital zircons from a sample (SONIA 1)  
118 “from the Cordillera Darwin complex”, for which the youngest significant age peak  
119 spans 260–370 Ma. A statistically preferred calculated age of  $289.3 \pm 2.7$  Ma was  
120 interpreted as the best maximum depositional age; one grain gave a younger age  
121 of  $163 \pm 8$  Ma, which is “significantly younger than the other estimates and  
122 biostratigraphic and detrital-zircon maximum depositional ages for broadly  
123 equivalent metasedimentary units in the Patagonian Andes (Hervé & Fanning  
124 2003; Hervé *et al.* 2003)”. Nevertheless, part of the protolith of the CDMC includes  
125 Tobífera Formation rhyolites, particularly on the southern slope of Cordillera  
126 Darwin (along the Beagle Channel), where strongly deformed and metamorphosed  
127 rhyolite lenses appear to be tectonically interleaved with the metasedimentary  
128 basement units (Nelson *et al.* 1980).

129 The basement rocks of the CDMC are intruded by granitoid plutons, which  
130 Nelson (1981) grouped into two suites, confirmed by various dating methods: the  
131 foliated Mid Jurassic Darwin Suite ( $157 \pm 7$  Ma, Hervé *et al.* 1981;  $164 \pm 4$  Ma,  
132 Mukasa & Dalziel 1996) and the essentially post-metamorphic Cretaceous Beagle  
133 Suite (70–90 Ma; Kohn *et al.* 1995; Mukasa & Dalziel 1996). The former suite was

134 metamorphosed together with the CDMC basement in Late Cretaceous times  
135 (Kohn *et al.* 1995), the granites being transformed into orthogneisses and the  
136 mafic dykes that intrude them (considered as lateral equivalents of the mafic rocks  
137 of the Rocas Verdes Basin) into amphibolites. The protolith of the high-grade  
138 (staurolite and kyanite–sillimanite) metamorphic rocks of Cordillera Darwin could  
139 thus have been the Palaeozoic basement rocks, the Mesozoic cover rocks, or  
140 both.

141 North of Cordillera Darwin, U–Pb dating of basement samples from the  
142 bottom of oil-well boreholes drilled through the Cretaceous–Cenozoic sedimentary  
143 fill of the Magallanes foreland basin (Fig.1) establishes that the local basement  
144 includes Cambrian igneous and metamorphic rocks (Söllner *et al.* 2000; Pankhurst  
145 *et al.* 2003) below an erosional unconformity at the base of the Tobífera  
146 Formation. Thus, the basement complexes of the Magallanes Basin and of  
147 Cordillera Darwin appear to differ significantly in their ages and lithology; they  
148 were the depositional surface for the Tobífera Formation in both areas, but their  
149 mutual contact relationships are not exposed.

150 We have determined U–Pb SHRIMP ages on detrital zircons from  
151 metasedimentary rocks from the CDMC in an attempt to resolve their depositional  
152 ages and to examine their possible provenance from the adjacent Ediacaran to  
153 earliest Cambrian basement of eastern Tierra del Fuego. Detrital zircon ages were  
154 also obtained from three low-grade metasedimentary rocks from the basal unit of  
155 the unconformably overlying Tobífera Formation, and from a granitic clast included  
156 in them, as further constraints on the age of the CDMC from which they were  
157 derived. Magmatic protolith ages were also determined on two metamorphic  
158 borehole samples from Lago Mercedes (see Fig. 1).

159

## 160 **Methodology**

161

162 Field work was carried out during four seasons of boat cruises in the area. After  
163 petrographical inspection of over 100 samples, 20 were selected for isotopic  
164 analysis. Zircon concentrates were prepared at the Departamento de Geología,  
165 Universidad de Chile. The U–Pb ages determined during this investigation were  
166 obtained using SHRIMPs I, II and RG at the Research School of Earth Sciences,  
167 The Australian National University, Canberra. The measurement techniques are  
168 similar to those of Williams (1998) and Hervé *et al.* (2003). Cathodoluminescence  
169 (CL) images were used throughout to select areas for analysis. In the case of the  
170 detrital zircon analyses, CL images were used to locate the youngest component  
171 within any single zircon grain. Representative CL images of zircon grains analysed  
172 are given with the electronic supplementary material. The Temora reference zircon  
173 (Black *et al.* 2003) was used to calibrate the U/Pb ratios, except for samples  
174 FO0508, FO0524 and FO0545 where the Duluth Gabbro FC1 zircon was used  
175 (Paces & Miller 1993). The data were processed using SQUID Excel Macro of  
176 Ludwig (2001), plots and age calculations have been made using ISOPLOT  
177 (Ludwig 2003) incorporating the mixture modelling algorithm of Sambridge &  
178 Compston (1994). The number of grains analysed varied depending on whether  
179 the sample was for age determination or for provenance (see figures and the

180 supplementary material for the number of grains analysed for individual samples).  
181 For grains that were obviously older than 1000 Ma,  $^{204}\text{Pb}$ -corrected  $^{207}\text{Pb}/^{206}\text{Pb}$   
182 ages were preferred, whereas for the younger grains  $^{207}\text{Pb}$ -corrected  $^{238}\text{U}$ - $^{206}\text{Pb}$   
183 ages were considered more meaningful. Uncertainties are given as  $1\sigma$  on the  
184 analytical measurements in the supplementary material and as 95% confidence  
185 limits on all calculated weighted mean ages reported in this paper. The initial  
186 analyses of samples FO0508, FO0539 gave unexpected and anomalous Jurassic  
187 dates. Additional SHRIMP sessions were carried out to check these anomalies  
188 and carry out further analyses; for sample FO0508 a second piece of the same  
189 rock was separated at ANU. Results are summarized in Table 1 and plotted in  
190 Figs. 2 to 7 (the full U-Th-Pb data tabulation is given in the supplementary  
191 material). The geological time-scale used is that of IUGS-ICS 2009  
192 ([www.stratigraphy.org](http://www.stratigraphy.org)).  
193

## 194 **Analysed samples**

### 196 ***Basal Clastic Complex of the Tobífera Formation***

197  
198 Rocks of this complex, assigned to the base of the Tobífera Formation by Johnson  
199 (1990), crop out in the northern slope of Cordillera Darwin (Fig.1); they show only  
200 a faint foliation and weak metamorphism. Three arenite samples were collected at  
201 Seno Almirantazgo. FO0524 is a feldspathic litharenite cropping out at Puerto  
202 Demonio, Bahía Ainsworth, with quartz, plagioclase, slate/phyllite, quartzite and  
203 marble clasts. It is part of a succession in which clast-supported conglomerates  
204 containing 1–10 cm pebbles of quartz, micaschist and volcanic rocks predominate.  
205 FO0531 is a sub-litharenite with phyllite, quartz and quartzite clasts from Bahía  
206 Ainsworth; it is part of a succession where conglomeratic sandstones and quartz  
207 conglomerates predominate. The sandstones have shale laminae, cross-bedding,  
208 and 1–2 m thick conglomerate beds with channelized bases. FO0539 is a foliated  
209 quartzose phyllite from a conglomeratic succession at Puerto Hernández, Fiordo  
210 Brookes, which conformably underlies an ignimbrite bed dated at  $168.7 \pm 1.4$  Ma  
211 (unpublished data by the authors). Finally, FO0516 is a 10 cm diameter granitic  
212 clast from a matrix-supported foliated conglomerate bed at Fiordo Parry, with  
213 mainly aphanitic siliceous volcanic rock clasts.  
214

### 215 ***Cordillera Darwin Metamorphic Complex***

216  
217 We analysed three sets of samples from our Cordillera Darwin Metamorphic  
218 Complex collections. The first set (samples FO0508, FO0518, FO0622, FO0533)  
219 came from the northern flank of the cordillera around Seno Almirantazgo. The  
220 second set (FO0635 and FO0642) consists of samples from the Seno Searle  
221 region, to the southwest of the highest peaks of the cordillera. Finally, samples  
222 PIA1, PIA7C, GA17 and GA26 were collected from the fjords north of the Beagle  
223 Channel, along the southern flank of Cordillera Darwin. All locations are shown in  
224 Fig. 1 (GPS coordinates are given in the supplementary material).  
225

226 *Northern flank of Cordillera Darwin*: FO0508 is a quartz-rich amphibole-bearing  
227 foliated rock with seams rich in biotite, from Fiordo Parry. FO0518 is a schist with  
228 fine-grained bands consisting of quartz, biotite (including zircon with metamict  
229 halos), chlorite, traces of titanite and tourmaline, and quartz veinlets; it has a well  
230 developed crenulation cleavage. Ortiz (2007) determined the peak metamorphic  
231 conditions for rocks in this area, which include biotite-garnet bearing schists, at  
232 550–580°C and 5.0–5.4 kbar. A lower-temperature post-foliation metamorphic  
233 imprint can also be observed, mainly transforming biotite to chlorite. FO0622 is a  
234 mica-schist with small-scale folds, cropping out on the northern shore of Seno  
235 Keats, just below the unconformity with the Tobifera Formation. Nelson (1981)  
236 described the structure here as a major synclinal fold that allowed the preservation  
237 of the Tobifera. The sample contains detrital white micas and intensely folded  
238 quartz veins. FO0533 is a poly-deformed banded phyllite from Seno Ainsworth.  
239 The bands consist of granoblastic quartz, finer-grained plagioclase, coarser  
240 amphibole and epidote intergrowths, with minor biotite and garnet.

241  
242 *Southern flank of Cordillera Darwin*: Samples labelled PIA were collected at Bahía  
243 Pia, in the garnet–staurolite zone of the amphibolite facies metamorphic rocks of  
244 the CDMC. PIA1 is a staurolite-bearing quartz-biotite schist and PIA7C is a  
245 kyanite-bearing schist (Alvarez 2007). Samples labelled GA were collected from  
246 Seno Garibaldi from biotite-grade metamorphic rocks (Alvarez 2007): GA17 is a  
247 rhyolitic dyke intruding the metamorphic basement in the Schists Unit (Alvarez  
248 2007), and GA26 a poly-deformed silicic volcanic rock.

249  
250 *South-western Cordillera Darwin (Seno Searle)*: FO0635 is a weakly foliated white  
251 mica–biotite metapelite from Seno Searle. It is interlayered with greenschist and  
252 rocks interpreted in the field as silicic tuffs. FO0642 is a poorly foliated hornfelsic  
253 quartzite, consisting of an aggregate of fine-grained quartz, plagioclase and  
254 chloritized biotite, with epidote-bearing veinlets, from the northern shore of Seno  
255 Searle. The outcrop displays small-scale shear zones and is intruded by mafic  
256 dykes and a Jurassic diorite. Their locations are shown in Fig. 1.

### 257 258 ***Northwest of Cordillera Darwin***

259  
260 The basement rocks in this area are low-grade metasedimentary rocks. FO0545 is  
261 a grey banded phyllite with complexly folded bands rich in quartz, white mica and  
262 biotite, from a small island at the entrance of Seno Inman. FO0751 is a micaschist  
263 with abundant granoblastic quartz veins and aggregates, in bands of fine-grained  
264 quartz, white mica, chlorite, titanite with crenulation cleavage, and some coarser-  
265 grained white mica aggregates. FO0718 is a foliated carbonaceous metapelite  
266 with decussate biotite, white mica and quartz bands, with accessory tourmaline  
267 crystals and secondary white mica-bearing veins. FO0701, from the northern  
268 shore of the Strait of Magellan, is a quartzite with relict detrital texture, with quartz  
269 and plagioclase clasts in a foliated fine-grained quartz, white mica, chlorite, and  
270 epidote matrix; there are pressure-solution seams of opaque minerals, and  
271 pressure shadows around some of the clasts.

272

### 273 ***Basement of the Magallanes foreland basin***

274

275 Samples LM1 and LM2 were provided by Empresa Nacional del Petróleo (ENAP)  
276 and came from the bottom of two deep exploration boreholes at Lago Mercedes,  
277 Tierra del Fuego, 60 km north of Seno Almirantazgo (Fig. 1). LM1 is a foliated  
278 amphibolite and LM2 a banded orthogneiss.

279

### 280 **Results**

281

282 The analytical data are presented in Table 1 (supplementary material), and in  
283 Figures 2 to 7. All calculated ages are reported with 95% confidence limit  
284 uncertainties. For close comparison, ages reported from previous literature are  
285 quoted with  $2\sigma$  uncertainties.

286

### 287 ***Basal Clastic Complex of the Tobífera Formation***

288

289 The detrital age distribution of sandstone FO0524 exhibits a predominant broad  
290 peak which can be unmixed into two components, *c.* 530 and *c.* 550 Ma, both  
291 Cambrian in age (see relative probability plots, Fig.2). Scattered ages in the range  
292 350–470 Ma are subordinate to Permian ages, with a more prominent group at *c.*  
293 270 Ma and a smaller one at *c.* 245 Ma. Neoproterozoic grains are scarce.  
294 Sandstone FO0531 has a predominant and well defined younger peak at  $163.0 \pm$   
295  $1.7$  Ma (8 analyses, MSWD = 1.02), with subdued Permian (*c.* 280 Ma),  
296 Carboniferous (*c.* 345 Ma) and Cambrian (*c.* 545 Ma) peaks. A very minor group of  
297 1.0–1.2 Ga is seen within a wide dispersion of Proterozoic ages. The quartzose  
298 phyllite FO0539 records a wide range of detrital zircon ages, but with dominant  
299 Carboniferous peaks at  $337.2 \pm 3.9$  Ma (11 grains, MSWD = 0.84) and *c.* 360 Ma  
300 (5 grains). Also present are Grenville-age peaks (*c.* 1030 Ma and *c.* 1100 Ma, 6  
301 grains in each case), and a smaller late Neoproterozoic one (*c.* 615 Ma, 4 grains),  
302 with scattered Late Cambrian–Early Ordovician and Early Devonian ages also  
303 recorded. Two grains record Jurassic dates; a second analysis of the original  
304 single grain is reproduced and another also recorded during follow-up analyses in  
305 second SHRIMP analytical session. Lastly, the granite clast FO0516 has a single  
306 population of zoned igneous zircon. Two of the analysed grains appear to have  
307 lost radiogenic Pb, but the remaining 18 give a weighted mean  $^{206}\text{Pb}/^{238}\text{U}$  age of  
308  $465.6 \pm 3.2$  Ma (MSWD= 1.08), which is interpreted as the Mid Ordovician age of  
309 granite crystallization.

310

### 311 ***Cordillera Darwin Metamorphic Complex***

312

313 *Northern flank of Cordillera Darwin (Fig. 3).* Amphibole-bearing schist FO0508 is  
314 dominated by detrital zircons at around 400 Ma; 43 analyses from the 122 grains  
315 analysed are within uncertainty of a weighted mean  $^{206}\text{Pb}/^{238}\text{U}$  age of  $404.1 \pm 5.2$   
316 Ma (MSWD = 1.7). There are 8 analyses (from 6 grains) that are within uncertainty  
317 of a younger peak at  $166 \pm 2$  Ma (MSWD = 1.14) – these ages come from grains

318 that are predominantly igneous in origin. A second separation of this sample was  
319 made, but no Jurassic ages were identified from the 50 grains analysed. Some  
320 scattered early Palaeozoic ages are recorded, but the main pre-Devonian  
321 provenance is from 600–680 Ma sources.

322 Sample FO0518 shows two ill-defined main groupings around 600 Ma (500  
323 to 750 Ma) and around 1000 Ma (800 to 1200 Ma) with a tail to 2600 Ma of  
324 Mesoproterozoic to Archaean grains.

325 Micaschist FO0622 shows a zircon age spectrum (ignoring spot #28.1, c. 110  
326 Ma) that is characterized by numerous peaks or groupings, but with no stand-  
327 alone significant age grouping. There are two peaks at c. 385 and c. 405 Ma, an  
328 age gap, then a series of approximately equal, closely-spaced peaks at c. 510, c.  
329 530, c. 565, c. 600 and c. 620 Ma. A broad Meso-Neoproterozoic range of ages is  
330 observed with a more prominent peak at about 1040 Ma, as well as some  
331 Palaeoproterozoic grains (1880–2000 Ma).

332 The data for phyllite FO0533 show a dominant concentration at 440–480 Ma,  
333 with a dominant age defined by 12 grains at  $450.2 \pm 4.6$  Ma (MSWD = 0.76) and a  
334 subordinate group at  $473.1 \pm 5.3$  Ma (10 analyses, MSWD = 0.92). Eight grains  
335 have ages between 560 and 670 Ma, and further nine between 985 and 1150 Ma.  
336 There is a significant presence of earliest Palaeoproterozoic and Archaean grains,  
337 with 13 having ages between 2460 and 2660 Ma, and a sub-peak at about 2620  
338 Ma.

339  
340 *Southern flank of Cordillera Darwin (Fig. 4).* The staurolite-bearing schist sample  
341 PIA1 yielded relatively few zircons; they range up to 100 $\mu$ m in length though many  
342 are less than 50  $\mu$ m. They are round to sub-round, elongate to equant in shape,  
343 and exhibit both zoned igneous and more homogeneous CL structure, the latter  
344 interpreted as metamorphic. The relative probability plot is characterized by a  
345 number of closely spaced age peaks, seemingly a continuum from c. 300 Ma to c.  
346 700 Ma, with other groupings at 880 to 900 Ma and c. 975 to c. 1180 Ma. There  
347 are some scattered older Palaeoproterozoic ages. For the 300–700 Ma age range,  
348 small but significant peaks occur at c. 330, c. 430, c. 465, c. 520 and c. 560 Ma,  
349 with subordinate clusters of Brasiliano ages (approximately 650–700 Ma). No  
350 zircon grains younger than c. 300 Ma were recorded.

351 The relative probability distribution of ages for kyanite schist PIA7C also  
352 shows a range of peaks, mainly between c. 480 Ma and c. 630 Ma. The most  
353 prominent peaks are at c. 480 Ma and c. 520 Ma, and lesser ones at c. 550 Ma, c.  
354 590 Ma and c. 630 Ma. There are scattered older grains, some with Brasiliano  
355 ages between c. 630 and c. 710 Ma, as well as a spread of 'Grenvillian' ages, and  
356 three grains with Palaeoproterozoic and Archaean ages.

357 The rhyolite dyke GA17 contains a relatively uniform population of euhedral,  
358 prismatic zircons that have a simple zoned igneous internal structure under CL  
359 imaging. The relative probability plot of  $^{206}\text{Pb}/^{238}\text{U}$  ages is skewed slightly to the  
360 older side; there also appears to have been some radiogenic Pb loss. A weighted  
361 mean of 16 of the 20 analyses gives  $159.1 \pm 1.4$  Ma (MSWD = 1.7) and this is  
362 interpreted as the time of zoned igneous zircon crystallization in the rhyolite dyke.  
363 GA26, a silicic volcanic rock, has a disparate population of zircons that range from

364 low-U (100–350 ppm) euhedral and oscillatory-zoned igneous zircon to extremely  
365 high-U (up to 13,850 ppm), dark to opaque, metamict zircon. The latter constitute  
366 the majority of the grains in the heavy mineral concentrate and were mostly not  
367 suitable for analysis; moreover, the SHRIMP U/Pb ratio calibration does not hold  
368 well for such extreme U contents (Williams & Hergt 2000), so that the variable  
369 ages obtained from the few analysed high-U grains are not considered reliable.  
370 The low-U grains tend to group at about 155 Ma and this is the likely time of zoned  
371 igneous zircon formation.

372  
373 *South-western Cordillera Darwin (Seno Searle)(Fig. 5)*. Metapelite FO0635, from  
374 which 70 zircon grains were analysed, displays a predominant peak at c. 130 Ma  
375 (Early Cretaceous), a Permian peak at c. 270 Ma, a smaller peak at c. 370 Ma;  
376 there are dispersed grains in the interval 430 to 555 Ma (Silurian to latest  
377 Proterozoic), a small peak at 460 Ma (Ordovician), and a few scattered  
378 Proterozoic grains.

379 Permian zircons were also found in quartzite FO0642, with 26 of 60 analysed  
380 grains recording ages between 255 and 300 Ma; these can be sub-divided, a  
381 group of 9 grains yielding a mean age of c. 260 Ma, a second group of 11 grains  
382 yielding c. 275 Ma and a third group of 6 grains yielding c. 290 Ma. Among the  
383 older ages, there is a minor Carboniferous group at about 320 Ma and then a  
384 continuum from c. 385 to 520 Ma, albeit with 6 ages concentrated around c. 485  
385 Ma (Early Ordovician). Some scattered Neoproterozoic ages are also present.

386

### 387 ***Northwest of Cordillera Darwin***

388

389 Grey banded phyllite FO0545 shows a very wide range of detrital zircon ages, with  
390 many between 490 and 700 Ma (Fig. 6). Isolated grains younger than 490 Ma are  
391 interpreted as having lost radiogenic Pb and are not considered further in this  
392 discussion. There is a prominent group of 11 analyses within uncertainty of  $596 \pm$   
393  $6$  Ma and a subordinate group of 6 analyses at  $504 \pm 6$  Ma, with lesser groupings  
394 around c. 540 and c. 630 Ma. A significant group of 15 grains with ages between  
395 950 and 1150 Ma indicates a component of Grenville-age provenance, with an  
396 apparent peak at c. 1045 Ma. Some Palaeoproterozoic and Archaean grains are  
397 also present, but in isolation their significance is difficult to interpret.

398 The areas analysed from the quartz-rich micaschist FO0751 from Bahia Morris  
399 are enriched in common Pb and this seems to be a mount-related problem and  
400 leads to a scattered Tera-Wasserburg plot (not shown). However, the  $^{204}\text{Pb}$ -  
401 corrected Grenville-age and older grains are within uncertainty of concordia, so the  
402 corrected  $^{206}\text{Pb}/^{238}\text{U}$  ratios are probably reasonable, at least for the main peaks.  
403 The peaks include a predominant latest Proterozoic one, with minor groupings and  
404 individual ages from Late Proterozoic to Archaean.

405 The areas analysed from FO0718 on the same mount as FO0751 are  
406 similarly enriched in common Pb. The  $^{204}\text{Pb}$ -corrected Grenville-age and older  
407 grains are within uncertainty of concordia, and for the younger grains the corrected  
408  $^{206}\text{Pb}/^{238}\text{U}$  ratios are probably reasonable. The latter dominantly give Permian

409 dates and the weighted mean for 26 grains is  $277 \pm 3$  Ma, with a subordinate  
410 slightly older grouping close to 290–295 Ma.

411 Sample FO0701 is dominated by Carboniferous zircons. There is a broad  
412 concentration of data at around 300–360 Ma, with two possible peaks unmixed at  
413 about 330 and 345 Ma, but it is not possible to identify any specific major events.  
414

### 415 ***Basement of the Magallanes foreland basin***

416  
417 Banded amphibolite sample LM1 has a population of relatively coarse-grained,  
418 homogeneous glassy zircon, with broad internal CL zoning commonly seen in  
419 igneous zircons from gabbroic rocks (see supplementary material). A large  
420 number of grains were analysed and the relative probability plot shows a dominant  
421 single age peak, with a significant tail on the younger side, interpreted as due to  
422 loss of radiogenic Pb during metamorphism of this basic igneous rock. The well-  
423 defined Cambrian weighted mean  $^{206}\text{Pb}/^{238}\text{U}$  age of  $527.2 \pm 5.2$  Ma (MSWD = 1.5,  
424 60 grains out of 72; Fig. 7) is interpreted as the time of igneous zircon  
425 crystallization in the pre-metamorphic protolith. Sample LM2 (granitic orthogneiss)  
426 is also dominated by igneous zircon occurring as elongate grains up to 100–  
427 200 $\mu\text{m}$  in length with oscillatory-zoned interiors. The relative probability plot shows  
428 a dominant age peak with a tail on the younger side and a series of younger U-Pb  
429 ages. From the Tera-Wasserburg plot, these younger analyses are interpreted as  
430 areas that have lost radiogenic Pb (grain 4 has 5,300 ppm U and has clearly lost  
431 radiogenic Pb). The main group yields a well-defined weighted mean  $^{206}\text{Pb}/^{238}\text{U}$   
432 age of  $536.8 \pm 3.3$  Ma (MSWD = 1.4, 39 grains out of 60; Fig.6), giving the time of  
433 zoned igneous zircon crystallization.  
434

### 435 **Discussion**

#### 437 ***Identifying basement and cover in the CDMC***

438  
439 Since one of the main goals of this contribution was to investigate the nature, age  
440 and provenance of the CDMC, it was first necessary to establish reliable criteria to  
441 separate the basement and cover, as metamorphosed “cover” (of Jurassic–Lower  
442 Cretaceous rocks) is an important component of the CDMC. Clearly, those  
443 metamorphic rocks analysed that contain Jurassic and/or Cretaceous zircons were  
444 most probably part of the cover sequences. This obviously applies to the BCC  
445 sample FO0531, but could also include sample FO0508, which was collected from  
446 an area mapped as basement but which contains rare grains of zoned igneous  
447 zircon, clearly not related to a post-depositional *in situ* metamorphic event. The  
448 interpretation that best matches the data is that this amphibolite-grade rock is a  
449 metamorphosed age-equivalent of the BCC. A similar situation may be  
450 represented by sample SONIA1 analysed by Barbeau *et al.* (2009), which was  
451 collected from an area shown as basement on their Figure 1 but as Tobífera  
452 Formation on our map (based on SERNAGEOMIN 2002). The possibility that  
453 rocks such as these are equivalents of the BCC rather than part of the CDMC  
454 basement unit proper illustrates the difficulty of distinguishing the two where

455 deformation is high. It also emphasizes that in such widespread metamorphic  
456 terrains it is not always possible to confidently assign outcrops to specific mapped  
457 units; in some ways better insight may be obtained through detailed isotope  
458 studies such as herein. The mid-to-Late Cretaceous high-grade metamorphism  
459 might well have affected these Jurassic (early Cretaceous?) rocks and erased the  
460 original structural fabric of the protolith, although this has remained recognisable,  
461 for example, in the Jurassic rhyolites and dyke (samples GA17, GA26) at Seno  
462 Garibaldi, where metamorphic grade is lower. In the south-western part of the  
463 Cordillera Darwin, at Seno Searle, metapelites with zircons of Cretaceous ages  
464 (FO0635) have been deformed, metamorphosed and incorporated in the CDMC,  
465 but their metamorphic grade is, once more, lower than in most of the CDMC.  
466 These rocks probably are metamorphosed equivalents of the Yaghan Formation,  
467 and thus belong to the cover of the CDMC.

468 The presence of Jurassic zircon grains cannot be considered the only  
469 trustworthy distinguishing criterion, since such grains are not recorded in all BCC  
470 samples. However, the analysed BCC samples (except FO0539) consistently  
471 record Permian detrital zircon age peaks, whereas in most of the samples clearly  
472 assigned to the CDMC basement the youngest detrital zircon population is  
473 Carboniferous in age. We thus consider, as a working principle, that CDMC rocks  
474 with Permian and younger zircon populations represent part of the Cordillera  
475 Darwin cover sequence and samples with older zircon age spectra are part of the  
476 CDMC basement.

477 It was not possible during this research to identify and date basement  
478 igneous rocks, whose existence has been previously indicated (e.g., Hervé *et al.*  
479 1981)

480

### 481 ***The basements of the CDMC and of the Magallanes foreland basin: two*** 482 ***distinct terranes?***

483

484 Detrital zircon age spectra from metasedimentary rocks considered as part of the  
485 CDMC basement, according to the above mentioned criteria, show mainly early  
486 Palaeozoic, Proterozoic and even Archaean peaks. The dominant Palaeozoic  
487 peaks differ between individual samples: 500 Ma (Late Cambrian) in FO0545, 480  
488 Ma (Early Ordovician) in PIA7C, 450 Ma (Late Ordovician) in FO0533, and 400–  
489 405 Ma (Early Devonian) in FO0508 and FO0622. Together with the Precambrian  
490 detritus, these spectra indicate a mixture of igneous sources derived from different  
491 parts of Gondwana. It is possible that detrital zircons in this area had a source in  
492 Laurentia, and we cannot rule out the idea that there was a collision between  
493 Gondwana and Laurentia near the Proterozoic–Phanerozoic boundary (e.g.,  
494 Dalziel 1997, Dalla Salda *et al.* 1992).

495 Cambrian detrital zircons are not very abundant in the three samples from  
496 the northern CDMC, but significant in those from the south. Additionally, the latter  
497 also have sizeable Ordovician peaks of c. 470–480 Ma, an age usually associated  
498 with the Famatinian orogenic belt that extends from north-western Argentina as far  
499 south as the North Patagonian Massif, but hitherto unknown from southern  
500 Patagonia. Yet, the  $465.6 \pm 3.2$  Ma age for the FO0516 granite clast from the

501 Basal Clastic Complex implies that igneous rocks of this age were exposed  
502 reasonably close to the Cordillera Darwin region during the Jurassic.

503 The youngest significant zircon grains in each sample give maximum early  
504 Palaeozoic (Ordovician to Devonian) ages for their deposition. These ages vary  
505 considerably between different samples. Despite some uncertainties over possible  
506 radiogenic Pb-loss, maximum sedimentation ages may be assigned as Early  
507 Devonian for FO0508, Late Ordovician for FO0533, Early Ordovician (ca. 490 Ma)  
508 for FO0545, and mid-Ordovician for the host rock of FO0516. In the first two cases  
509 the dominance of the younger peaks over older ages could be taken to suggest  
510 erosion of a penecontemporaneous magmatic arc. On the southern flank of the  
511 CDMC, sample PIA7C has minimum zircon ages of 405 Ma (Early Devonian), but  
512 also has single-grain ages extending into the Carboniferous (ca. 365 and 340 Ma).  
513 PIA1 has a significant Early Carboniferous peak at c. 330 Ma. Since the  
514 significance of single-grain based ages may not be reliable, we suggest that the  
515 patterns presented indicate deposition mainly during the Early Palaeozoic in the  
516 north and Late Palaeozoic in the southern slope of Cordillera Darwin.

517 The SHRIMP U-Pb zircon age spectra of rocks from the basement of the  
518 Magallanes foreland basin collected from the oil wells at Lago Mercedes differ  
519 significantly from those of the Cordillera Darwin Metamorphic Complex. The well-  
520 defined Early Cambrian ages of the former are interpreted here as crystallization  
521 ages of igneous rocks, i.e., the protoliths of the present-day foliated gneiss and  
522 amphibolites. Foliated granitoids of c. 530 Ma have previously been demonstrated  
523 to underlie the Tobífera Formation of northern Tierra del Fuego (Söllner *et al.*  
524 2000; Pankhurst *et al.* 2003) and are part of the Tierra del Fuego Igneous and  
525 Metamorphic Complex (TFIMC; Hervé *et al.* in revision); together with our new  
526 data, this suggests that such Cambrian igneous rocks are widespread in the  
527 basement of the Magallanes Basin. The scarcity of Cambrian detrital zircons in the  
528 CDMC is at odds with the occurrence of extensive Cambrian orthogneisses and  
529 amphibolites in the basement of central and northern Tierra del Fuego. It might be  
530 expected that these Cambrian rocks should be one the most likely candidates to  
531 provide detrital zircons for CDMC protolith in the early Palaeozoic, as is the case  
532 with samples FO0545 and FO0751. However, significant Cambrian detrital zircon  
533 populations appeared in sedimentary rock of the Cordillera Darwin region only in  
534 the Jurassic, when the “Basal Clastic Complex” was deposited unconformably  
535 over the CDMC at Seno Almirantazgo.

536 Thus, according to standard definitions (Howell 1989), the basements of the  
537 Magallanes foreland basin and the CDMC constitute two separate and distinct  
538 tectonostratigraphic terranes. The basement of the Magallanes foreland basin is  
539 currently found 4 km below sea level, whereas that of the CDMC crops out at up to  
540 2 km above sea level. These two basement terranes lie respectively to the north  
541 and south of the left-lateral Magallanes–Fagnano transform fault system (MFFS,  
542 Fig. 1), which forms the boundary between the Scotia and South American plates;  
543 the CDMC is located within the Scotia plate and the Fuegian foreland in the South  
544 American plate. Although strike-slip motion along the Magallanes Fagnano  
545 transform during the Cenozoic may explain the juxtaposition of the two terranes,  
546 estimated displacement along the transform boundary seems to be rather modest

547 (55 km according to Rossello 2005). This, together with the fact that the  
548 distribution of Jurassic and younger units and early Cenozoic structures can be  
549 matched across the fault regardless of displacement, leads us to suggest that the  
550 MFFS possibly resulted from the reactivation of an old, pre-Jurassic suture  
551 between the Cordillera Darwin and Tierra del Fuego basement terranes. The two  
552 terranes amalgamated before the deposition of the Basal Clastic Complex.  
553

### 554 ***Regional correlations of the CDMC basement***

555

556 The data presented here can be interpreted as indicating that the clastic protolith  
557 of the CDMC basement was not mainly derived from the presently adjacent,  
558 though buried, igneous/metamorphic basement of the Magallanes foreland basin.  
559 Furthermore, the zircon age spectra for most of the CDMC basement samples  
560 make untenable earlier correlations with the Madre de Dios Terrane that forms  
561 part of the western Patagonian archipelagos, north of the Strait of Magellan, as the  
562 latter includes clastic metasediments (Duque de York Complex; Forsythe &  
563 Mpodozis 1979, 1983; Sepúlveda *et al.* 2007) characterized by prominent Permian  
564 detrital zircons (Hervé *et al.* 2003). However, one sample (FO0642) from the  
565 strongly tectonized Seno Searle region, the south-westernmost locality sampled,  
566 and sample FO0718, northwest of Cordillera Darwin have a youngest prominent  
567 Permian peak, so that these samples might represent either fragments of the  
568 Duque de York Complex or younger sediments tectonically interleaved with the  
569 CDMC basement, and deformed and metamorphosed together during the  
570 Cretaceous. Despite this, most CDMC basement samples are more comparable in  
571 their detrital zircon age spectra to some samples of the Eastern Andes  
572 Metamorphic Complex. This complex crops out along the eastern Andean foothills  
573 north of 50°S (Hervé *et al.* 2003; Augustsson & Bahlburg 2007; Hervé *et al.* 2008),  
574 and was considered by Hervé and Mpodozis (2005) as an exotic terrane (Fitz Roy  
575 terrane) accreted against southern Patagonia in, probably, early Jurassic times.  
576 Notwithstanding these similarities, at present the Cordillera Darwin basement  
577 cannot be considered an integral part of the former as the intervening Cambrian  
578 meta-igneous terrane of Tierra del Fuego disrupts the geographic continuity of  
579 these two separate tectonic domains.  
580

### 581 **Conclusions**

582

583 The metasedimentary basement unit present in the Cordillera Darwin Metamorphic  
584 Complex, characterized by mainly Early Palaeozoic detrital zircons as the  
585 youngest components, differs from the Cambrian meta-igneous basement of the  
586 Magallanes foreland basin. It also differs from the Duque de York Complex, part of  
587 the Madre de Dios Terrane, in that samples of the latter have a prominent Early  
588 Permian detrital zircon component. The detrital zircon patterns of the CDMC are  
589 more comparable to those of the Eastern Andes Metamorphic Complex further  
590 north in the Patagonian Andes, interpreted as having been deposited in a passive  
591 margin setting. However, at present, both areas are spatially separated by the  
592 Cambrian meta-igneous basement of the Magallanes foreland basin in Tierra del

593 Fuego, and they cannot be considered to form a continuous rock body. The  
594 presence of Ordovician detrital zircons and granitic clasts complicates the  
595 identification of the source areas, as granites of such ages are not known in  
596 southern Patagonia.

597 The CDMC lies in the Scotia Plate, whose Cenozoic boundary with the South  
598 America plate is the left lateral wrench Magallanes–Fagnano fault system (MFFS).  
599 The detrital zircon patterns of the CDMC basement unit are more complex than if  
600 they had the exclusively Cambrian igneous source of the presently adjacent  
601 Magallanes foreland basin basement. This suggests that the two areas were not  
602 side-by-side during the Early Palaeozoic, but that their amalgamation occurred  
603 prior to the Middle Jurassic, as indicated by Jurassic Tobífera volcanic rocks  
604 unconformably deposited over both basements. The MFFS was thus probably  
605 developed along the site of an older suture, located in the contact between the  
606 CDMC and the meta-igneous Cambrian Magallanes foreland basin basement.

607 Jurassic detrital zircons are present in some samples of the CDMC, including  
608 some from outcrops assigned to the basement in some maps; their zircon age  
609 patterns resemble those in the sedimentary rocks that lie unconformably over the  
610 basement unit of the CDMC and concordantly below the Tobífera Formation. Thus  
611 zircon data and field relationships are consistent in showing that the CDMC cover  
612 units were deposited in Jurassic times and were deformed and metamorphosed to  
613 high grades along with the CDMC basement during Cretaceous times.

614

## 615 **Acknowledgements**

616

617 Field trips were undertaken in the yachts *Penguin* and *Foam*, with captains  
618 Conrado Alvarez and David Lleufo. Additionally, a field trip in southern Cordillera  
619 Darwin by KK was made on the *Ocean Tramp* with Captain Charles Porter.  
620 Projects FONDECYT 1050431 and 7050431 (FH), Anillo-Antártico (ARTG-04),  
621 and NSF EAR0635940 (KK) financed most of the field and laboratory work. M.  
622 Ortiz, A. Sanchez, C.F. Prades, F. Poblete and J. Alvarez, geology students from  
623 Universidad de Chile, were excellent field collaborators. KK also thanks Prof.  
624 Geoffrey Clarke from the University of Sydney for his assistance in the field during  
625 the *Ocean Tramp* cruise. RJP acknowledges assistance with travel costs by  
626 NERC Isotope Geosciences Laboratory. Thorough reviews by D. Barbeau and an  
627 anonymous referee helped to greatly improve the original text.

628

## 629 **References**

630

631 Allen, R.B. 1982. Geología de la Cordillera Sarmiento, Andes Patagónicos, entre  
632 los 51°00' y 52°15' Lat. S., Magallanes, Chile. Servicio Nacional de Geología y  
633 Minería Boletín, Santiago 38, 46.

634

635 Alvarez, J. 2007. *Evolución geodinámica del Complejo Metamórfico Cordillera*  
636 *Darwin, Tierra del Fuego, XII Región, Chile*. Unpublished Thesis, Departamento  
637 de Geología, Universidad de Chile, 79 p, Santiago.

638

639 Augustsson, C. & Bahlburg, H. 2007. International Journal of Earth Sciences  
640 (Geologische Rundschau) DOI 10.1007/s00531-006-0158-7.  
641

642 Barbeau, D.L.Jr., Olivero, E.B., Swanson-Hysell, N.L., Zahid, K.M., Murray, K.E. &  
643 Gehrels, G.E. 2009. Detrital-zircon geochronology of the eastern Magallanes  
644 foreland basin: implications for Eocene kinematics of the northern Scotia Arc and  
645 Drake Passage. *Earth & Planetary Science Letters*, 284, 489-503.  
646

647 Black, L.P., Kamo, S.L., Allen, C.M., Aleinikoff, J.N., Davis, D.W., Korsch, R.J. &  
648 Foudoulis, C. 2003. TEMORA 1: a new zircon standard for Phanerozoic U–Pb  
649 geochronology. *Chemical Geology*, 200, 155-170.  
650

651 Calderón, M., Hervé, F., Massonne, H.-J., Tassinari, C. G., Pankhurst, R. J.,  
652 Godoy, E. & Theye, T. 2007a. Petrogenesis of the Puerto Edén Igneous and  
653 Metamorphic Complex, Magallanes, Chile: Late Jurassic anatexis of  
654 metagreywackes and granitoid magma genesis. *Lithos*, 93, 17-38.  
655

656 Calderón, M., Fildani, A., Hervé, F., Fanning, C.M., Weislogel, A. & Cordani, U.  
657 2007b. Late Jurassic bimodal magmatism in the northern seafloor remnant  
658 of the Rocas Verdes basin, southern Patagonian Andes. *Journal of the Geological  
659 Society, London*, 164, 1011-1022.  
660

661 Dalla Salda, L., Cingolani, C. & Varela, R. 1992. Early Paleozoic orogenic belt of  
662 the Andes in southwestern South America: result of Laurentia – Gondwana  
663 collision? *Geology*, 20, 617-620.  
664

665 Dalziel, I.W.D. 1981. Back-arc extension in the Southern Andes: a review and  
666 critical reappraisal. *Philosophical Transactions of the Royal Society of London*,  
667 A300, 319-335.  
668

669 Dalziel, I.W.D. 1986. Collision and Cordilleran orogenesis : an Andean  
670 perspective. In: Coward, M.P. & Ries, A.C. (eds) *Collision Tectonics*. Geological  
671 Society, London, Special Publications, 19, 389–404.  
672

673 Dalziel, I.W.D. & Cortés, R. 1972. Tectonic style of the southernmost Andes and  
674 the Antarctandes. 24th International Geological Congress, Section 3, 316–327.  
675

676 Dalziel, I.W.D., de Wit, M.J. & Palmer, K.F. 1974. Fossil marginal basin in the  
677 southern Andes. *Nature*, 250, 291-294.  
678

679 Dalziel, I.W.D. & Brown, R.L. 1989. Tectonic denudation of the Darwin  
680 metamorphic core complex in the Andes of Tierra del Fuego, southernmost Chile :  
681 implications for Cordilleran orogenesis. *Geology*, 699-703.  
682

683 Dalziel, I.W.D. 1997. Overview of Neoproterozoic-Paleozoic geography and  
684 tectonics: review, hypothesis and environmental speculation. *Geological Society of*

685 *America Bulletin*, 109,16-42.  
686  
687 Fildani, A., Cope, T., Graham, S.A. & Wooden, J. 2003. Initiation of the  
688 Magallanes foreland basin: timing of the southernmost Patagonian Andes orogeny  
689 revised by detrital zircon provenance analysis. *Geology*, 31, 1081-1084.  
690  
691 Forsythe, R.D. & Mpodozis, C. 1979. El Archipiélago de Madre de Dios, Patagonia  
692 Occidental, Magallanes: rasgos generales de la estratigrafía y estructura del  
693 basamento pre-Jurásico Superior. *Revista Geológica de Chile*, 7, 13-29.  
694  
695 Forsythe, R.D. & Mpodozis, C. 1983. Geología del Basamento pre-Jurásico  
696 Superior en el Archipiélago Madre de Dios, Magallanes, Chile. Servicio Nacional  
697 de Geología y Minería, Boletín 39, 63 p.  
698  
699 Hervé, F., Nelson, E., Kawashita, K. & Suárez, M. 1981. New isotopic ages and  
700 the timing of orogenic events in the Cordillera Darwin, southernmost Chilean  
701 Andes. *Earth & Planetary Science Letters*, 55, 257-265.  
702  
703 Hervé, F., Calderón, M. & Faundez, V. 2008. The metamorphic complexes of the  
704 Patagonian and Fuegian Andes. *Geologica Acta*, 6 (1), 43 – 53.  
705  
706 Hervé, F., Fanning, C.M. & Pankhurst, R.J. 2003. Detrital Zircon Age Patterns and  
707 Provenance in the metamorphic complexes of Southern Chile. *Journal of South  
708 American Earth Sciences*, Vol.16, 107-123.  
709  
710 Hervé, F. & Mpodozis, C. 2005. The western Patagonia terrane collage: new facts  
711 and some thought-provoking possibilities. In *Gondwana-12: Geological and  
712 Biological heritage of Gondwana* (Pankhurst, R.J. and Veiga, G.D., editors),  
713 Abstracts, p. 196. Mendoza, Argentina.  
714  
715 Hervé, F., Calderón, M., Fanning, C.M., Kraus, S., Pankhurst, R.J. (in revision).  
716 The age, nature and significance of the basement rocks of the Magallanes basin in  
717 Tierra del Fuego. *Andean Geology*.  
718  
719 Howell, D.G. 1989. *Tectonics of suspect terranes. Mountain building and  
720 continental growth*. 232 p., Chapman and Hall, London and New York.  
721  
722 Johnson, C. 1990. *Antecedentes estratigráficos de la ribera Sur del Seno  
723 Almirantazgo*. Unpublished Thesis, Departamento de Geología, Universidad de  
724 Chile, 122 p, Santiago.  
725  
726 Katz, H. R. & Watters, W. A. 1966. Geological investigation of the Yahgan  
727 Formation (Upper Mesozoic) and associated igneous rocks of Navarino Island,  
728 Southern Chile. *New Zealand Journal of Geology and Geophysics*, 9, 323-59.  
729

730 Kohn, M. J., Spear, F.S., Harrison, T.M. & Dalziel, I.W.D. 1995.  $^{40}\text{Ar}/^{39}\text{Ar}$   
731 geochronology and P-T-t paths from the Cordillera Darwin Metamorphic Complex,  
732 Tierra del Fuego, Chile. *Journal of Metamorphic Geology*, 13, 251-270.  
733

734 Ludwig, K.R. 2003. User's manual for Isoplot/Ex, Version 3.0, A geochronological  
735 toolkit for Microsoft Excel. Berkeley Geochronology Center Special Publication No.  
736 4, 2455 Ridge Road, Berkeley CA 94709, USA.  
737

738 Ludwig, K.R. 2001. SQUID 1.02, A User's Manual, Berkeley Geochronology  
739 Center Special Publication. No. 2, 2455 Ridge Road, Berkeley, CA 94709, USA.  
740

741 Mukasa, S.B. & Dalziel, I.W.D. 1996. Southernmost Andes and South Georgia  
742 Island, North Scotia Ridge: Zircon U-Pb and muscovite  $^{40}\text{Ar}/^{39}\text{Ar}$  age constraints  
743 on tectonic evolution of Southwestern Gondwanaland. *Journal of South American*  
744 *Earth Sciences*, 9, 349-365.  
745

746 Nelson, E. 1981. *Geologic Evolution of the Cordillera Darwin orogenic core*  
747 *complex, southern Andes*. PhD thesis, Columbia University, 142 p.  
748

749 Nelson, E., Dalziel, I. W. D. & Milnes, A. G. 1980. Structural geology of the  
750 Cordillera Darwin: Collision style orogenesis in the southernmost Chilean Andes,  
751 *Eclogae Geologicae Helveticae*, 73, 727-751.  
752

753 Ortiz, M. 2007. *Condiciones de formación del Complejo Metamórfico Cordillera*  
754 *Darwin, al Sur de Seno Almirantazgo, Region de Magallanes , Chile*. Unpublished  
755 Thesis, Departamento de Geología, Universidad de Chile, 79 p, Santiago.  
756

757 Paces, J. B., & Miller, J. D. 1993. Precise U-Pb ages of Duluth Complex and  
758 related mafic intrusions, northeastern Minnesota: Geochronological insights to  
759 physical, petrogenetic, paleomagnetic, and tectonomagmatic process associated  
760 with the 1.1 Ga Midcontinent Rift System. *Journal of Geophysical Research*, 98,  
761 13,997-14,013.  
762

763 Pankhurst, R.J., Rapela, C.W., Laske, W.P., Márquez, M. & Fanning, C.M. 2003.  
764 Chronological study of the pre-Permian basement rocks of southern Patagonia.  
765 *Journal of South American Earth Sciences*, 16, 27-44.  
766

767 Rossello, E.A. 2005. Kinematics of the Andean sinistral wrenching along the  
768 Fagnano - Magallanes Fault Zone (Argentina - Chile Fueguian Foothills). 6<sup>th</sup>  
769 International Symposium on Andean Geodynamics, Barcelona, Actas 623 - 626.  
770

771 Sambridge, M.S. & Compston, W. 1994. Mixture modelling of multicomponent data  
772 sets with application to ion-probe zircon ages. *Earth and Planetary Science*  
773 *Letters*, 128, 373-390.  
774

775 Sepúlveda, F.A., Hervé, F., Calderón, M. & Lacassie, J.P. 2008. Petrology of  
776 igneous and metamorphic units from the allochthonous Madre de Dios Terrane,  
777 Magallanes, Chile. *Gondwana Research* 13 (2): 238-249.  
778  
779 SERNAGEOMIN 2002. Mapa Geológico de Chile, escala 1: 1.000.000. Servicio  
780 Nacional de Geología y Minería, Santiago, Chile.  
781  
782 Söllner, F., Miller, H. & Hervé, M. 2000. An Early Cambrian granodiorite age from  
783 the pre-Andean basement of Tierra del Fuego (Chile): the missing link between  
784 South America and Antarctica?, *Journal of South American Earth Sciences* 13,  
785 163-177.  
786  
787 Watters, W.A. 1964. Geological work at Puerto Edén, Wellington island, southern  
788 Chile. *Transactions of the Royal Society of New Zealand. Geology*, 2 (11), 155-  
789 168.  
790  
791 Williams, I.S. 1998. U–Th–Pb geochronology by Ion Microprobe. In: McKibben, M.  
792 A., Shanks, W.C.III & Ridley, W.I. (eds) *Applications of microanalytical techniques  
793 to understanding mineralizing processes. Reviews in Economic Geology*, 7, 1-35.  
794  
795 Williams, I.S. & Hergt, J.M. 2000. U–Pb dating of Tasmanian dolerites: a  
796 cautionary tale of SHRIMP analysis of high-U zircon. In: Woodhead, J.D., Hergt,  
797 J.M., Noble, W.P. (Eds.), *Beyond 2000. New frontiers in Isotope Geoscience.*  
798 *Abstracts and Proceedings*, Lorne, 185–188.  
799

800  
801  
802  
803  
804

### 805 **Figure captions**

806  
807 Figure 1. (A) Map indicating outcrop areas of metamorphic complexes in southern  
808 Patagonia and present day plate boundaries. (B) Geological sketch map of the  
809 Cordillera Darwin area, with indication of the sampling localities. Samples LM1 and  
810 LM2 are more than 4 km deep, the rest at sea level. BM, Bahía Morris; BP, Bahía  
811 Pia; BPI, Bahía Pluschow; CM, Caleta Murray; CW, Caleta Wood; FB, Fiordo  
812 Brookes; FP, Fiordo Parry; SA, Seno Ainsworth; SG, Seno Garibaldi; SI, Seno  
813 Inman; SK, Seno Keats; SS, Seno Searle; MFFS, Magallanes Fagnano Fault  
814 System.

815  
816 Figure 2. Three age vs. probability diagrams for samples from the Basal Clastic  
817 Complex (of the Tobífera formation) on the northern slope of Cordillera Darwin;  
818 inset plots are subsets for ages below 800 Ma. Lower right: Tera–Wasserburg  
819 diagram and inset of age vs. probability plot for the granitic clast (sample FO0516).  
820 NB, n is the number of analyses.

821

822 Figure 3. Age vs. probability diagrams for samples from the Cordillera Darwin  
823 Metamorphic Complex in the northern flank of Cordillera Darwin; inset plots are  
824 subsets for ages below 800 Ma. Note, n is the total number of analyses.

825

826 Figure 4. Three age vs. probability diagrams for samples from the Cordillera  
827 Darwin Metamorphic Complex in the southern flank of Cordillera Darwin; inset  
828 plots are subsets of the larger plots for ages below 800 Ma. Lower right: Tera-  
829 Wasserburg diagram and inset of age vs. probability plot for the metavolcanic rock  
830 (sample FO0516). Note, n is the total number of analyses.

831

832 Figure 5. Age vs. probability diagrams for samples from the Cordillera Darwin  
833 Metamorphic Complex in south-western Cordillera Darwin (Seno Searle); inset  
834 plots are subsets for ages below 800 Ma. Note, n is the total number of analyses

835

836 Figure 6. Age vs. probability diagrams for samples from the metamorphic  
837 basement to the northwest of Cordillera Darwin; inset plots are subsets for ages  
838 below 800 Ma. Note, n is the number of analyses.

839

840 Figure 7. Tera-Wasserburg and probability vs. age diagrams for samples LM1 and  
841 LM2 from the bottom of the Magallanes basin in the Lago Mercedes area; inset  
842 plots are subsets for ages below 800 Ma. Note, n is the number of analyses.

843

844 Figure 8. Multiple age histograms and probability plots for the different  
845 tectonostratigraphic units for the restricted age interval 100–800 Ma.

846

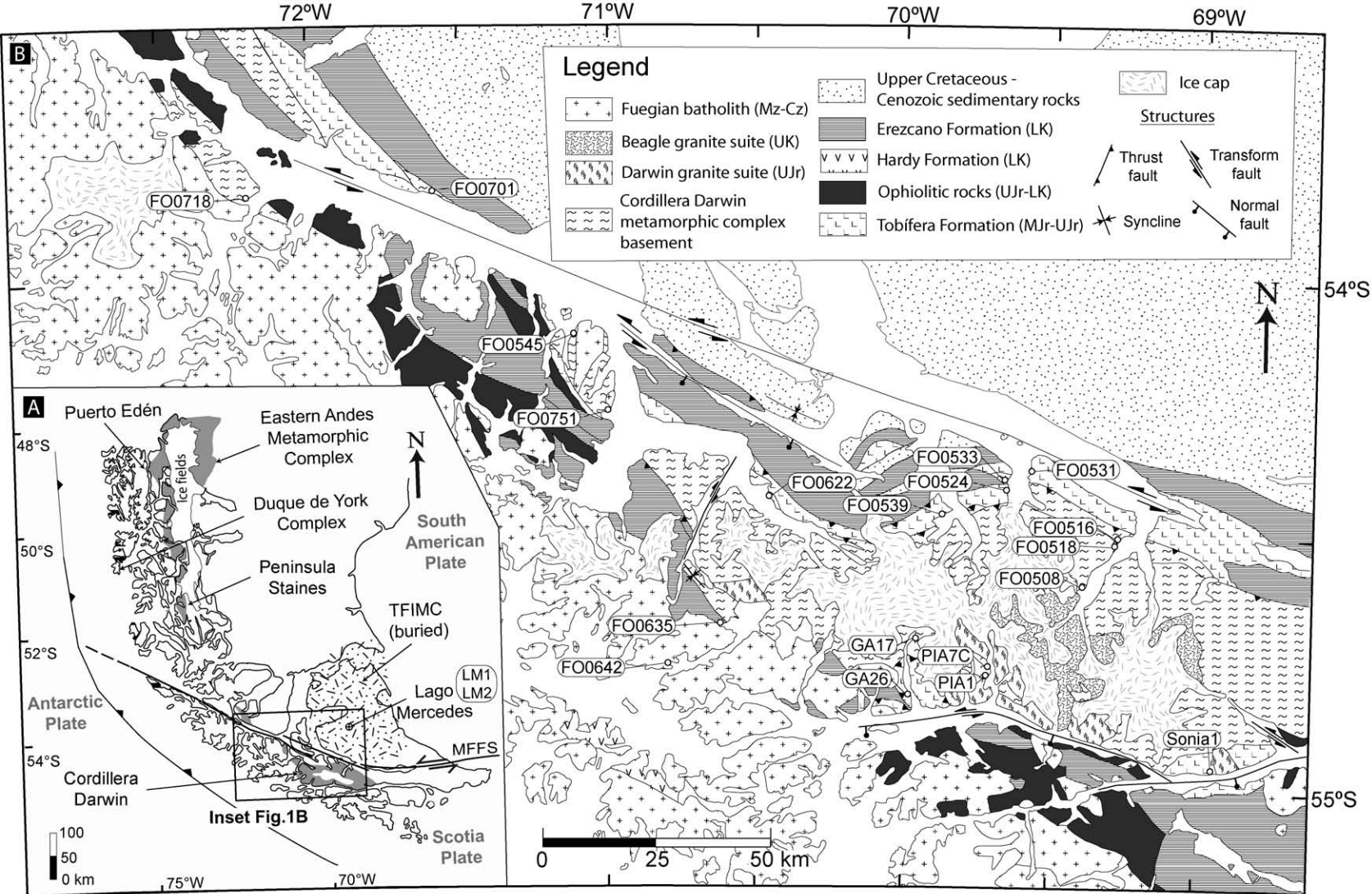


FIGURE 1. Hervé et al.

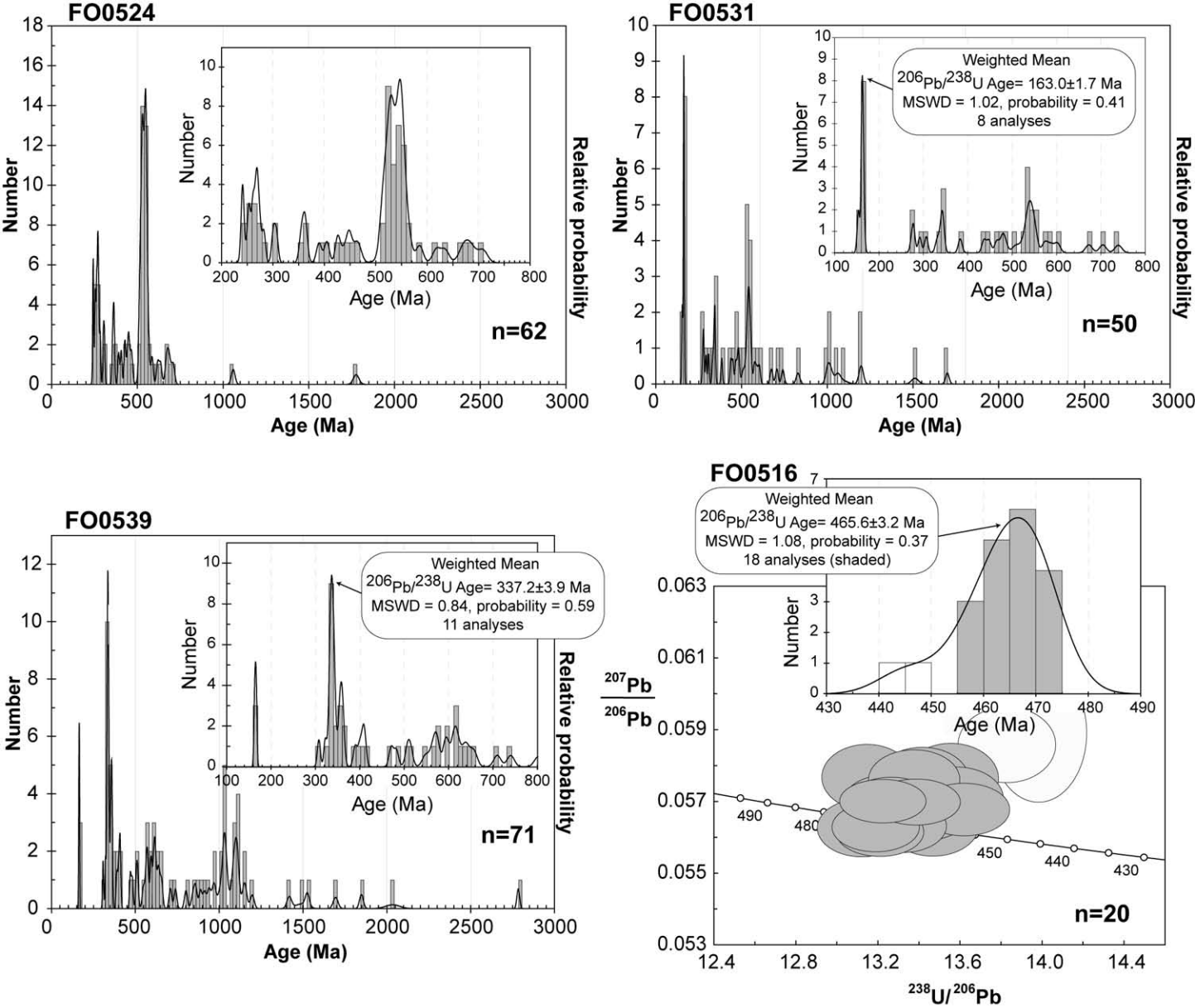


FIGURE 2. Hervé et al.

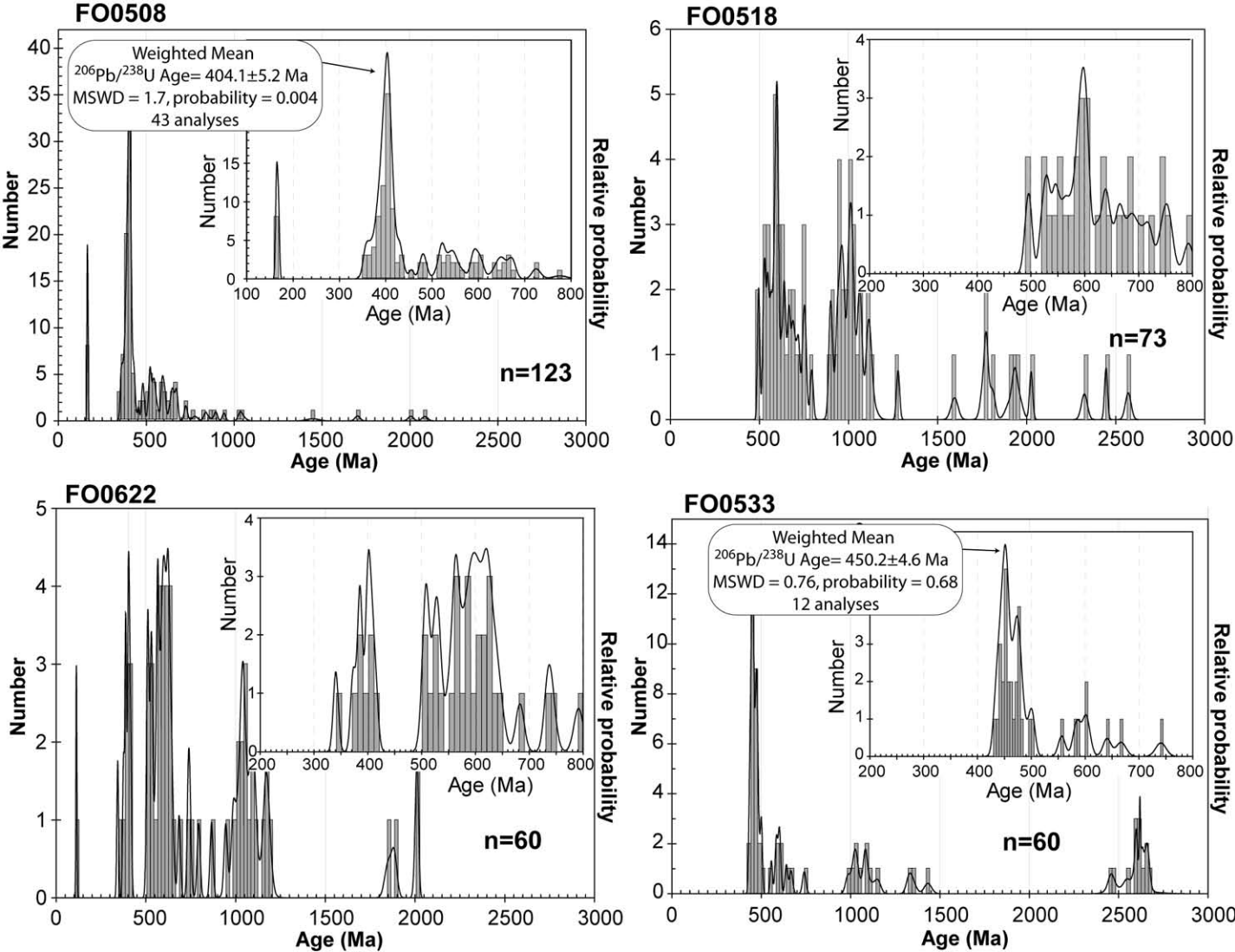


FIGURE 3. Hervé et al.

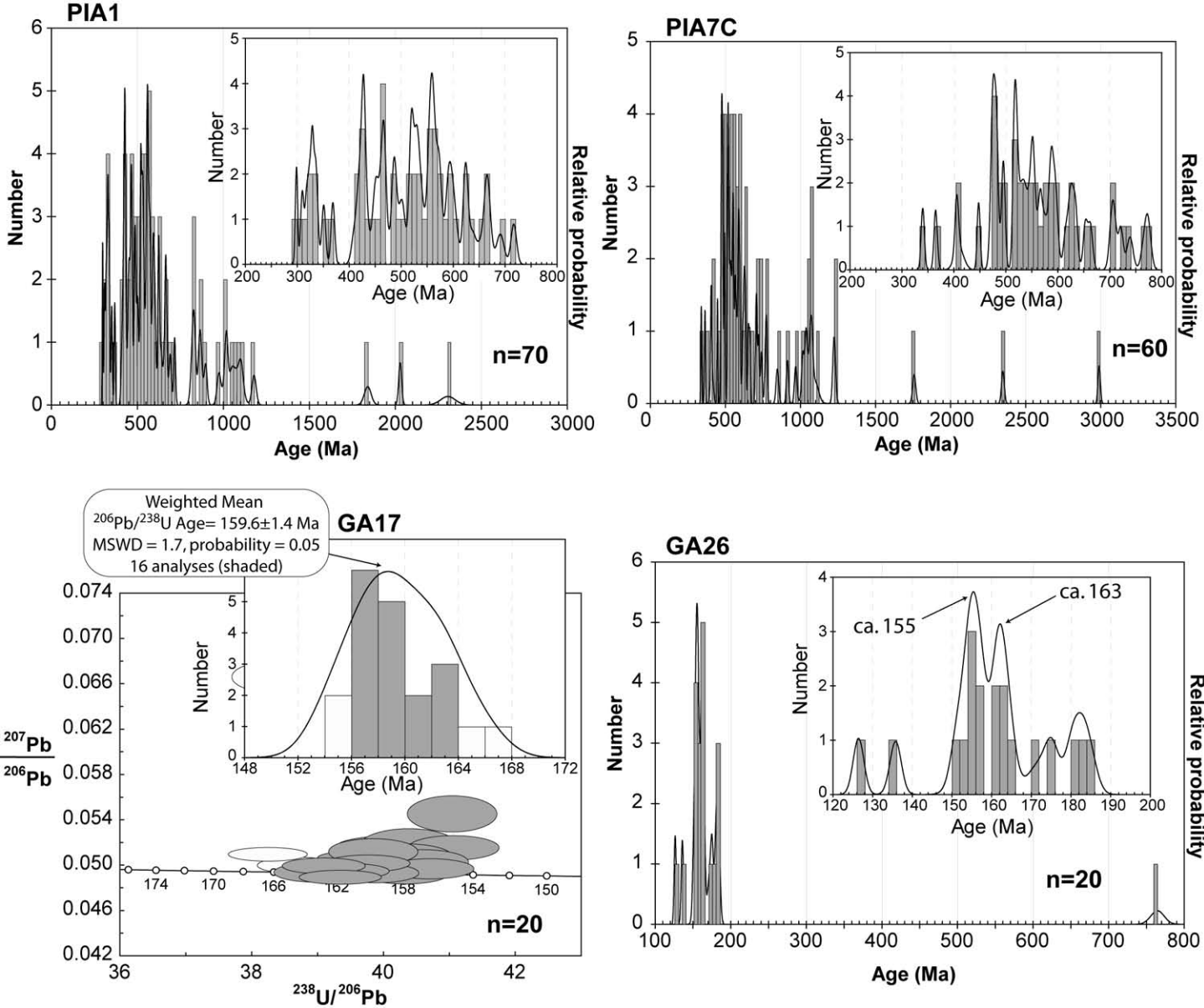


FIGURE 4. Hervé et al.

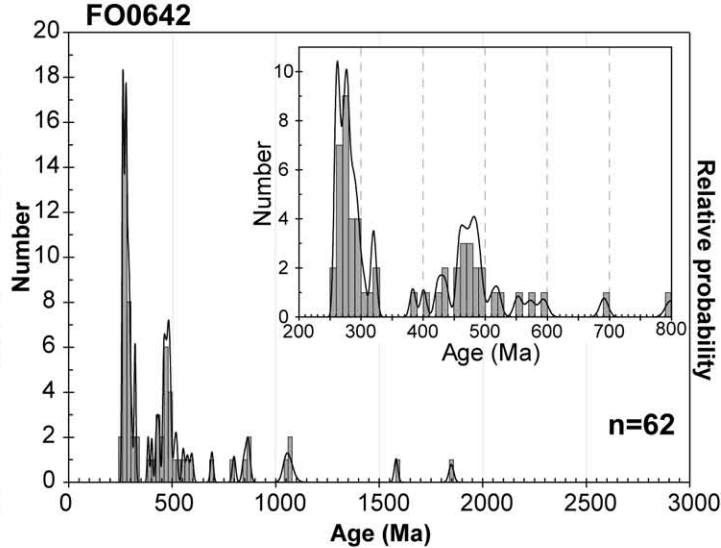
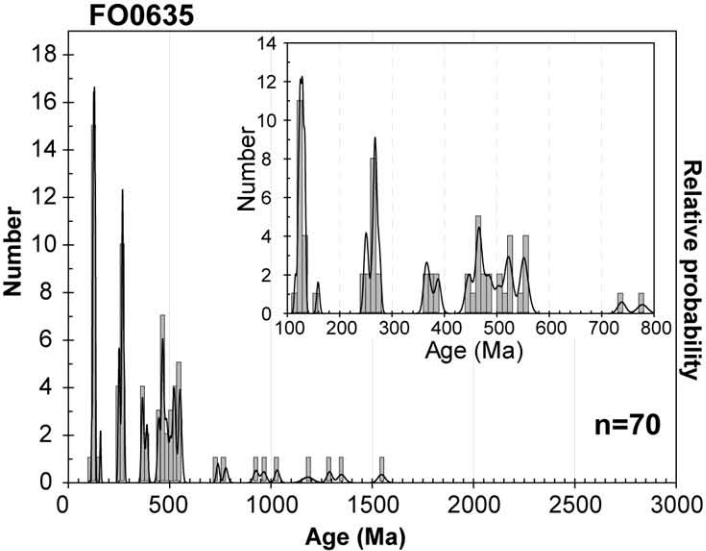


FIGURE 5. Hervé et al.

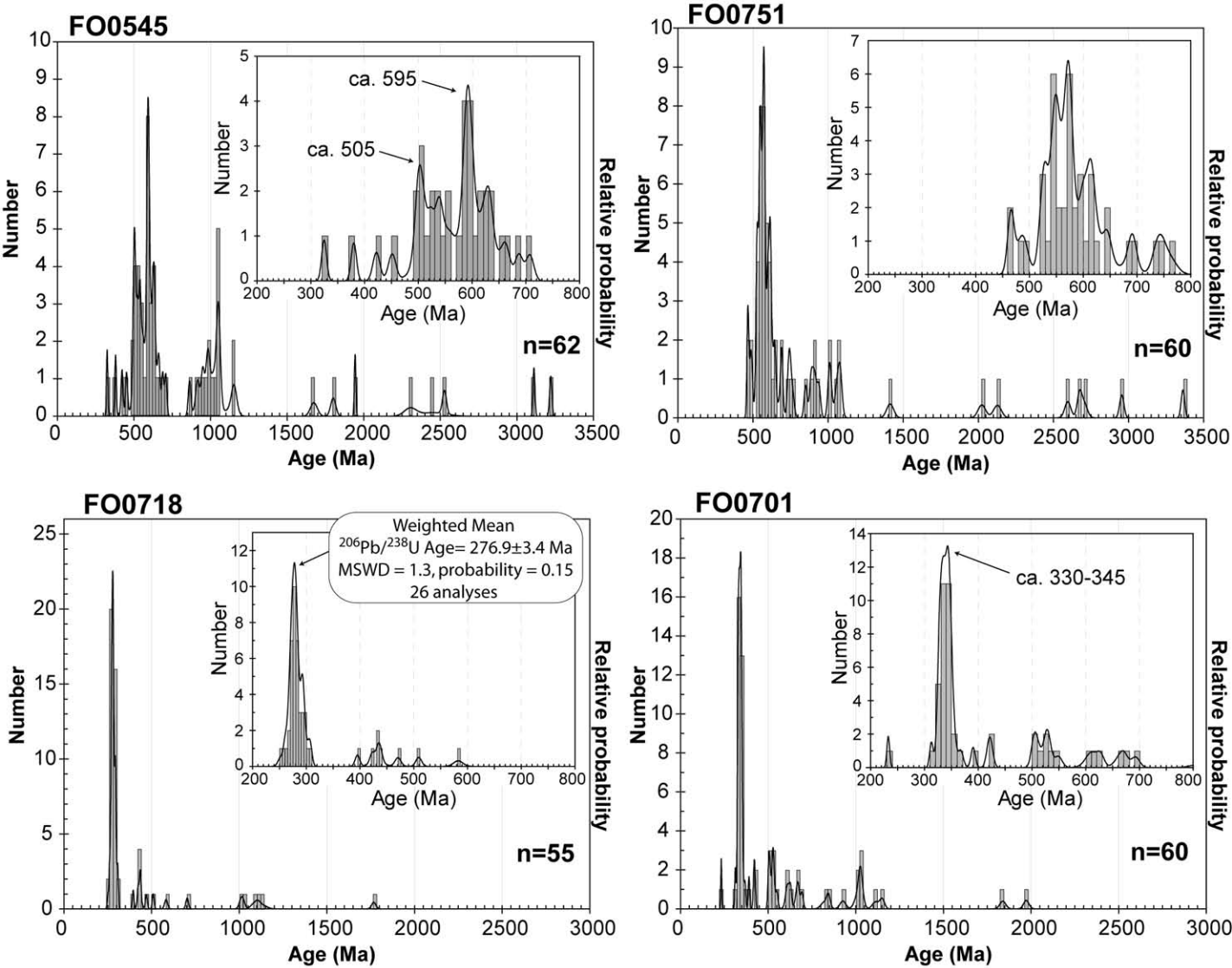


FIGURE 6. Hervé et al.

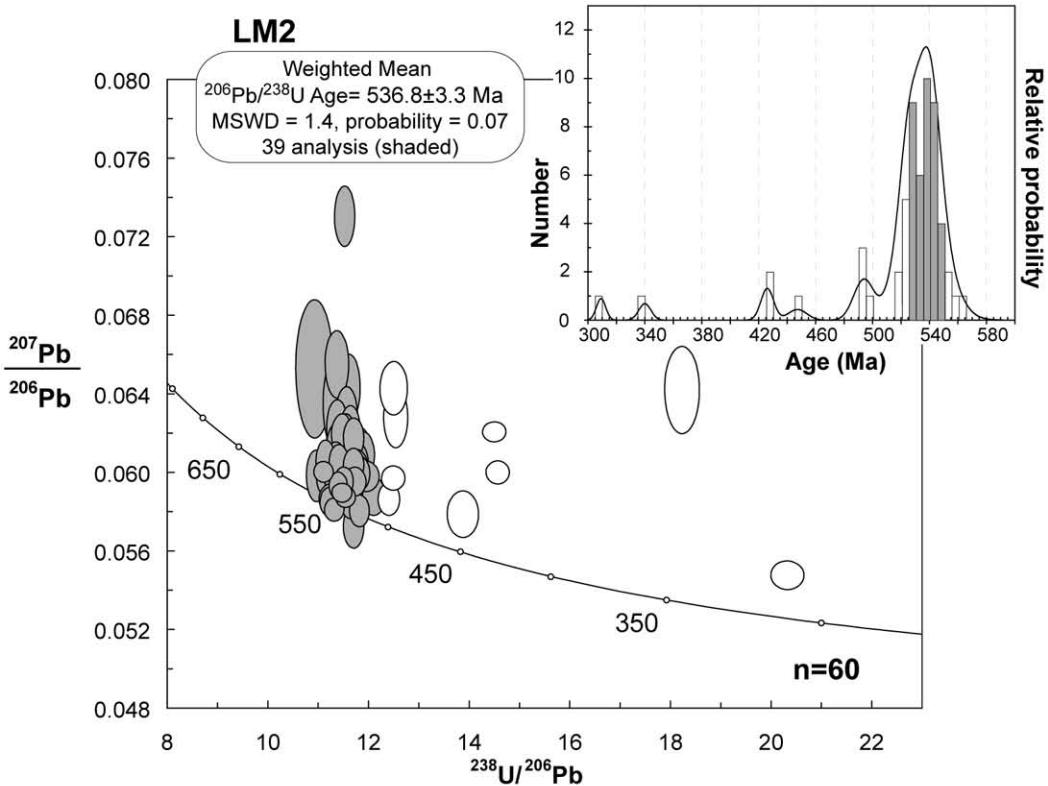
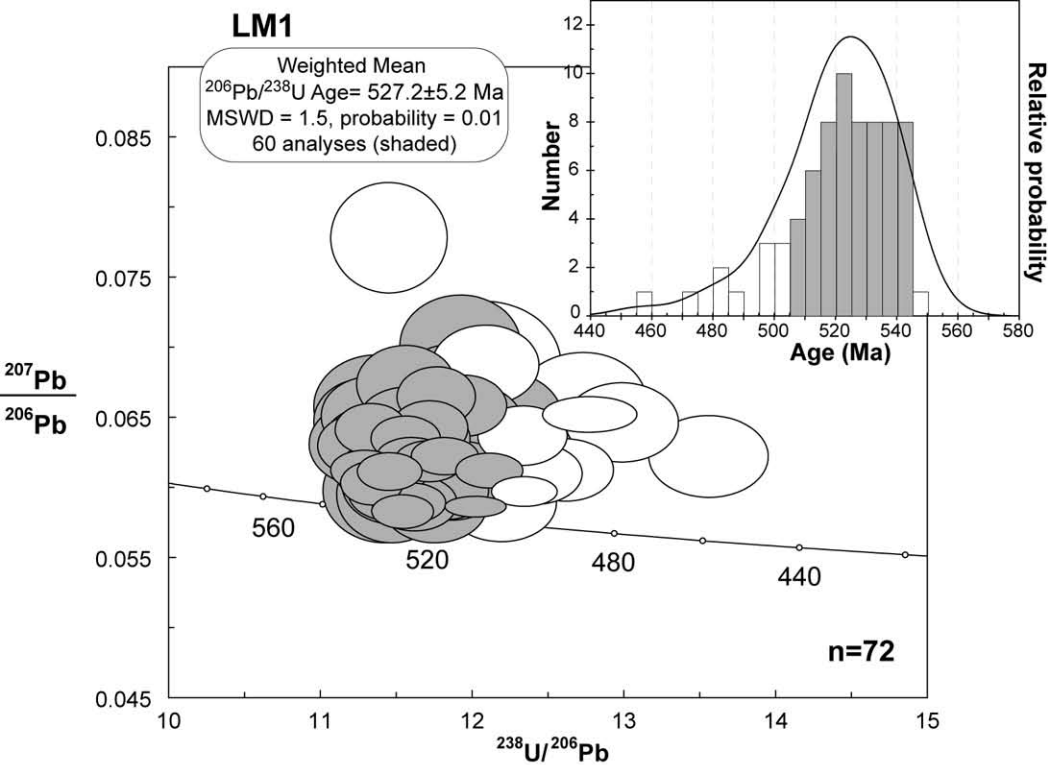


FIGURE 7. Hervé et al.

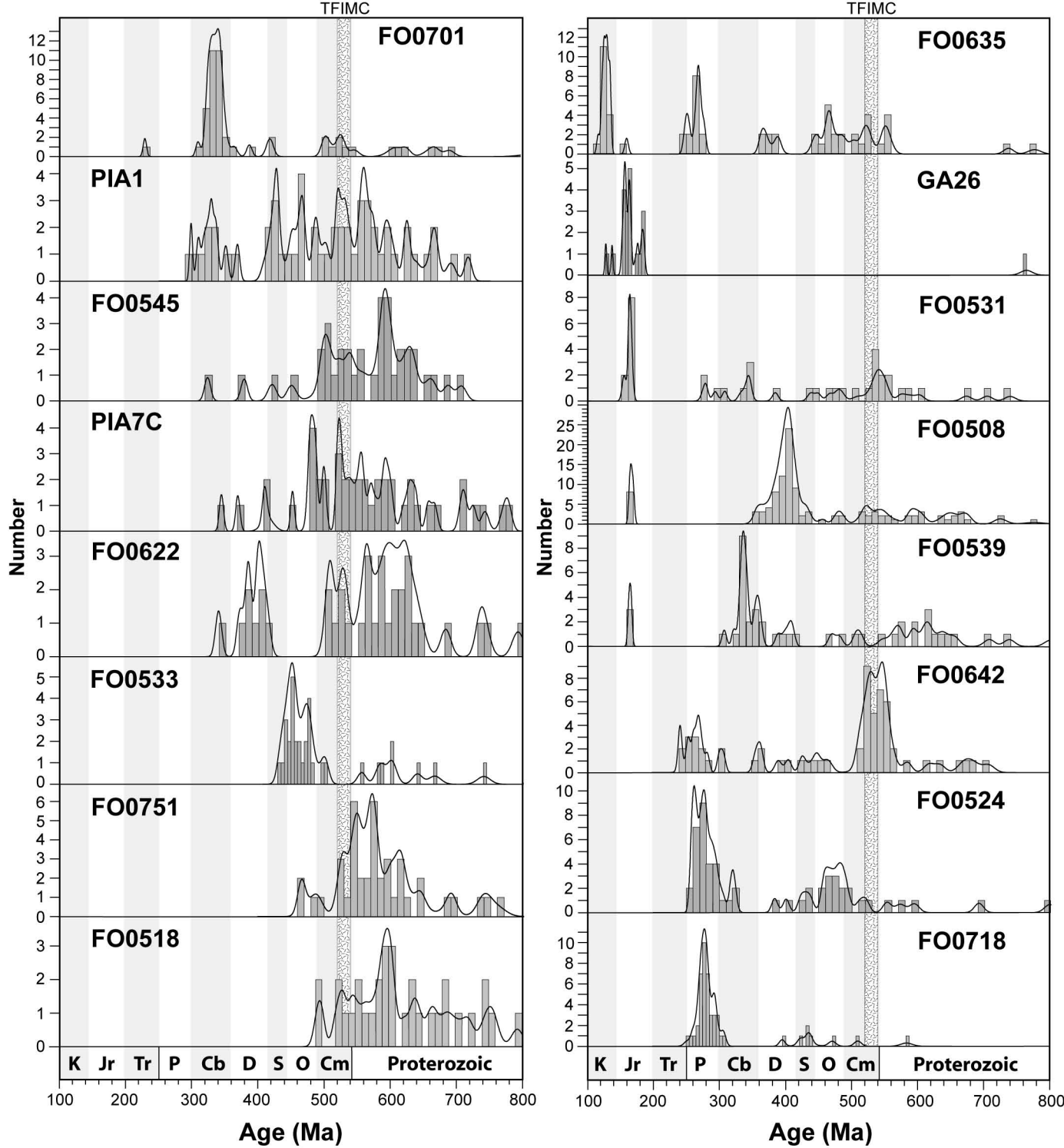


Figure 8. Hervé et al